Research on Engineering Structures & Materials
www.jresm.org

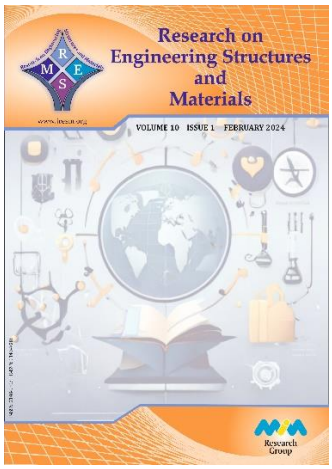

Growth of highly aligned ZnO nanorod arrays on zinc plates: Morphological and structural characterization

Berrin İkizler, Sümer M. Peker

Online Publication Date: 30 November 2023
URL: http://www.jresm.org/archive/resm2023.01ma1019rs.html
DOI: http://dx.doi.org/10.17515/resm2023.01ma1019rs

Journal Abbreviation: *Res. Eng. Struct. Mater.*

To cite this article
İkizler B, Peker M. Growth of highly aligned ZnO nanorod arrays on zinc plates: Morphological and structural characterization. *Res. Eng. Struct. Mater.*, 2024; 10(2): 623-636.

Research on Engineering Structures & Materials
www.jresm.org
MIM Research Group

Research Article

Growth of highly aligned ZnO nanorod arrays on zinc plates: Morphological and structural characterization

Berrin İkizler*[a], Sümer M. Peker[b]

Department of Chemical Engineering, Ege University, Bornova, İzmir, Turkey

Article Info

Article history:

Received 19 Oct 2023
Accepted 30 Nov 2023

Keywords:

ZnO nanorods;
Hydrothermal method;
Zinc substrate;
High alignment;
Seed layer;
Thermal oxidation

Abstract

In this work, uniform and highly aligned ZnO nanorod arrays were simply synthesized on zinc plates by hydrothermal method using zinc–ammonia complex solution. Effects of ZnO seed layer formation, $Zn(NO_3)_2$ concentration and $NH_3/Zn(NO_3)_2$ mole ratio (R) in the reaction medium on the morphology and crystal structure of nanorods were investigated in detail. ZnO nanorods grown on zinc surfaces were highly crystalline and had a hexagonal wurtzite structure, as revealed by XRD analysis. In addition, the dominant crystal growth direction was in *c*-axis, indicating the verticality of the nanorods. SEM images showed that one-dimensional (1D) ZnO nanorods with high verticality and number density were synthesized on seeded plates whereas randomly oriented arrays were grown on non-seeded surfaces. Increase in the Zn^{2+} concentration changed the top ends of the rods from tapering to hexagonal ends; and also led to an increase in the average size and verticality of the nanorods. The increase in R value (or i.e., amount of NH_3) caused the rods to misalign on the surface and decrease in size. The size of well-aligned nanorods can be adjusted from 50 to 260 nm in diameter and 0.11 to 6 μm in length by changing the reaction parameters, implying their large potential to be used in photocatalytic and also in electronic applications.

1. Introduction

ZnO is a naturally abundant, low cost and chemically stable n-type semiconductor, having a wide and direct band gap of 3.37 eV and a large excitonic binding energy of 60 meV [1-3]. It is distinguished by its properties such as its direct band gap energy, high electron mobility [3], being biocompatible [4], antibacterial [5] and low-toxic [5], and by also its tunable electrochemical [6], luminescence, magnetic, optical and electrical properties [7]. Therefore, ZnO is a promising material in applications such as, nanolasers [8], solar cells [9], gas sensors [10], photocatalysis [11], photoluminescence [4], transparent conductive films [12], energy efficient windows [13], field-emission devices, light-emitting diodes, acoustic wave filters, photonic crystals, photo-detectors, varistors, and piezoelectric materials [7,14].

The performance of ZnO nanoparticles in these applications is highly dependent on their shape, aspect ratio, surface cleanliness, and particle alignment. Also, orientation and interface quality affect the piezoelectric polarization, optical properties and charge carrier transportation properties of ZnO films [13,15]. The substrates coated with well-aligned ZnO nanorods or nanowires may exhibit much larger surface area than that of ZnO films prepared from randomly oriented nanoparticles. Besides, nanorods have higher electron transfer ability along their *c*-axis [16]. Therefore, well aligned one-dimensional (1D) array

*Corresponding author: berrin.ikizler@ege.edu.tr
[a] orcid.org/0000-0001-8889-0754; [b] orcid.org/0009-0009-5347-3884
DOI: http://dx.doi.org/10.17515/resm2023.01ma1019rs

coatings can be more preferred in the fields of electronics, solar cells or sensor applications [17,18].

ZnO nanoscale structures have been produced by methods such as molecular beam epitaxy, pulsed laser deposition, sputtering, anodic alumina oxide template, electrochemical deposition, vapor phase transport, chemical vapor deposition, thermal evaporation, sol-gel and hydrothermal method [1-14,19]. Among them, hydrothermal method is attractive due to its relatively low synthesis temperatures (<100°C) and low pressures, and it does not require complex experimental setups [8,20]. Therefore, the method has advantages such as simplicity, reproducibility, cost effectiveness, and suitability for large-scale production of thin films. Also, well-aligned and crystalline ZnO nanorod arrays can be synthesized by this method using a seeded template layer. Various substrates such as glass [20], ITO [2], aluminum membrane, crystalline quartz, polyethylene terephthalate (PET) wafer [12], carbon fiber, polycarbonate, poly(methyl methacrylate), and paper [3] have been used to grow ZnO nanorods. The growth process occurs in two steps on these surfaces: *(i)* formation of ZnO crystal seeds on the substrates; and *(ii)* synthesis of ZnO nanorods on these seeds by dipping into Zn^{2+} ion containing basic solution. Seeding substrates with ZnO creates sites for homogeneous nucleation of ZnO crystal during the synthesis. Common seeding methods include thermal decomposition of zinc acetate crystallites, spin/dip coating of ZnO nanoparticles and the use of various physical vapor deposition methods [2,17,21]. However, when the substrate is zinc, there is no need for a detailed precoating step before the growth stage [1,8,18,22]. Moreover, zinc foil is a conductive material with an electrical resistivity of 5.9×10^{-8} Ωm, making it facilely utilize the aligned ZnO nanorods for electronic, optoelectronic, and sensor devices. In addition, lattice matching between ZnO and Zn crystals facilitates the growth of a well-aligned ZnO nanorod array [23].

Hydrothermal method has been utilized to obtain ZnO nanostructures on the initially formed seeds by adjusting the reaction parameters. Yu et al. [17] synthesized well-aligned ZnO nanorod arrays on ITO substrates by first dip coating the surfaces with ZnO seed films. Zinc ion concentration and pH of reactions were changed, which revealed ZnO structures in the form of nanotubes, nanosheets, and nanorods with blanket-like shaped surfaces. Torres et al. [24] studied the nucleation and growth of ZnO nanorods on an ITO/PET substrate; and studied the effects of solution concentrations in both the seeding and hydrothermal treatment stages. They obtained ZnO nanorods with an average diameter of 50-195 nm, but not much perpendicular to the surface. The potential applications were stated as power generators and sensors. Lee et al. [1] grew ZnO nanorod arrays on Si substrate and zinc foil by changing the reaction time and thermal pretreatment period. They concluded that the use of zinc foil eliminated the need for ZnO nanoparticle seed layer, but orientation of the ZnO arrays seemed to be influenced negatively. ZnO nanorods were grown on the zinc foil also by Li et al. [21] without using any seed layer. They obtained aligned rods, but after a too long reaction time of 24 h. Yan et al. [23] synthesized ZnO nanorod arrays and flower-like ZnO nanosheets on zinc substrates by using a NaCl solution to accelerate the oxidation of zinc metal, but the process required a long reaction time of 16 h. Yue et al. [18] studied the growth of hierarchical ZnO arrays on zinc foil without the assistance of any seeds, catalysts and surfactants. The synthesized structure consisted of very thin nanosheets attached onto the top of nanorod arrays, but the process required a reaction period of 12 h at 120°C. Momeni [25] realized one-step synthesis of ZnO nanorods on zinc foils and found that their photocatalytic properties depend on the morphology of ZnO. Florica et al. [26] grew large-scale ZnO nanowires directly on zinc foils by thermal oxidation in air. They found that the oxidation temperature was effective on the density, diameter and length of the nanowires, but the alignment was not the focus of the work.

In the light of these findings, it can be stated that most of the studies in the literature focused on single-stage processes (usually applying oxidation in air or water) for the growth of ZnO nanorods on zinc foil. However, although different parameters (such as reaction time, concentration, annealing temperature, or different oxidation strategies, etc.) were investigated, randomly oriented nanorods were generally fabricated with the disadvantage of longer production times (up to 1 day in some studies). In another approach, ZnO nanorods were synthesized by hydrothermal treatment (<150°C) of zinc foils in basic zinc solutions, but the alignment of the rods still needs to be improved. Yet, to our knowledge, the growth of ZnO nanorods on zinc surfaces by combining oxidation and hydrothermal methods (a two-step process) to achieve high verticality has not been investigated, yet. Therefore, in this work, 1D nanorods were synthesized on zinc plates in two-steps: (i) first a seed layer is formed on the substrates by simply oxidizing in air, and then (ii) ZnO rods are grown on these seeds using hydrothermal method just only in 1.5 h within zinc-ammonia complex solution medium. Effects of preconditioning of the substrates, seed layer formation, $Zn(NO_3)_2$ concentration and $NH_3/Zn(NO_3)_2$ mole ratio were investigated in detail by means of the change in morphology and crystal structure of the synthesized ZnO nanorods. In our previous work, ZnO nanorod arrays were grown on glass surfaces, by investigating the effect of the thickness of the seed layer deposited by the spin coating method [27]. We found that chemical stability of ZnO nanorods (especially as photocatalysts) in aqueous media depends on rod verticality, and optimum seeding is a prerequisite for the well alignment. Differing from that work, in this study, zinc plate was used to grow well-aligned 1D ZnO nanorods, by performing a simple and one-step seeding process (i.e., thermal oxidation in air).

2. Materials and Methods

2.1. Materials

Zinc plates with a thickness of 0.5 mm were purchased from Ekmekçioğulları Industry&Trade Inc. (Turkey). The plates were cut into 20 mm × 20 mm dimension and used as the substrate. All chemicals used in the experiments were of analytical grade and purchased from Merck Co. Zinc nitrate hexahydrate ($Zn(NO_3)_2.6H_2O$, > 99%) was used as the Zn^{2+} ion source, and an aqueous ammonia solution (25 wt%), as the OH^- ion source to form nanorod growth solution. Pure water (18.2 MΩ.cm resistivity at 25°C) was used in the preparation of all solutions and obtained from the Millipore Direct-Q8-UV system.

2.2. Pretreatments Applied to the Zinc Substrates

(I) Cleaning: The substrates were subjected to ultrasonic cleaning sequentially in acetone, ethanol, and water (15 min with each solvent) to remove surface impurities before usage. *(II) Thermal oxidation in air (seed formation stage)*: The zinc plates were annealed at 300°C for 3 h and 6 h to produce a layer of ZnO seeds on the surface.

2.3. Growth of ZnO Nanorods on the Substrates

One-dimensional (1D) ZnO nanorods were grown on zinc plates by hydrothermal method using $Zn(OH)_4^{2-}$ complex solution as the reaction medium. The growth solution was prepared by mixing 50 mL of $Zn(NO_3)_2.6H_2O$ solution (in short, Zn^{2+} solution) with NH_3 solution. The molar ratio of NH_3 in this solution was adjusted as $R = n_{NH_3}/n_{Zn^{2+}}$ (see Table 1).

The zinc substrate, with (or without) a seed layer, was placed vertically into a Teflon-sealed stainless steel autoclave. The growth solution was then poured into the autoclave, and immediately the autoclave lid was tightly closed to prevent ammonia from escaping. Hydrothermal synthesis of ZnO nanorods on the surface was performed at a reaction

temperature of 90°C for 1.5 h. After that, the substrate was taken out from the autoclave and washed with water several times to remove the residual salt and amino complex from the surface. Then, it was left to dry under ambient conditions.

The effects of oxidation duration in the seed formation stage, existence of ZnO seed layer on the nanorod formation, concentration of Zn^{2+} and R ratio in the growth solution were investigated systematically (as given in Table 1) to improve the morphological and structural properties of the resultant ZnO nanorods.

Table 1. Investigated parameters, and their corresponding nanorod growth conditions

Parameters	Oxidation of Zn substrates	Nanorod growth conditions		
	Annealing time (h)	$[Zn^{2+}]$ (M)	$R = n_{NH_3}/n_{Zn^{2+}}$ (-)	Reaction time (h)
Oxidation duration	3	-	-	-
	6	-	-	-
ZnO seed layer formation	0	0.01	10	1.5
	3	0.01	10	
$[Zn^{2+}]$ in the growth solution	3	0.01	10	1.5
		0.05	10	
		0.10	10	
		0.15	10	
R ratio in the growth solution	3	0.10	7	1.5
		0.10	10	
		0.10	15	
		0.10	20	

2.4. Characterization

Field emission scanning electron microscopy (SEM, Phillips XL-30S FEG) operating at an accelerating voltage of 7 kV was used to observe the morphology of the ZnO nanorods. The shape, orientation, and dimensions (diameter-D, length-L, and aspect ratio-L/D) of the synthesized ZnO nanorods and also number density of rods over the surface were determined from SEM images using ImageTool-3.0 software. The crystal structure of the ZnO nanorod arrays were analyzed by X-ray diffraction (XRD, Phillips X'Pert Pro) using CuKα radiation for a 2 θ range of $5° - 90°$. X-ray wavelength of CuKα radiation is $\lambda =$ 0.15418 nm. The average grain (crystallite) sizes, D_c, were found from Scherrer equation [11],

$$D_c = (0.9\lambda)/(\beta \cos\theta) \quad (1)$$

where θ and β are Bragg's diffraction angle and full width at half-maximum (FWHM) value of (002) peak in radians, respectively. The (002) peak is the dominant characteristic peak of ZnO for nanorod structure since it describes the growth direction along *c*-axis. In the XRD results, peaks of zinc metal are shown by star (*).

3. Results and Discussion

3.1. Surface Structure of Zinc Substrates

The crystal structure and purity of zinc plates are assessed by XRD analysis, and the result is given in Fig. 1. The diffraction peaks at 36.2°, 38.9°, 43.1°, 54.2°, 69.9°, 70.5°, and 76.9° coincide well with the standard diffraction data of zinc with a JCPDS card no: 87-0713 [28]. The crystal planes corresponding to these peaks are shown in Fig. 1, and no peaks other

than Zn are detected in the diffraction peaks. Thus, it can be concluded that the substrates are pure zinc with hexagonal structure without any impurities.

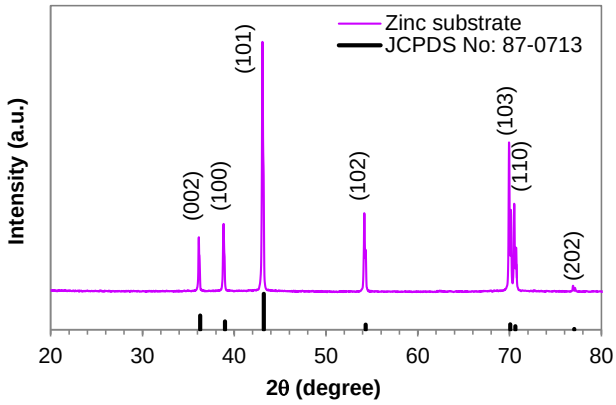

Fig. 1. XRD diffractogram of zinc plates

3.2. Oxidation of Zinc Substrates

Initial preconditioning of the substrates is critical for the growth of nanorod arrays [1,27]. Hence, the surfaces are commonly coated with a ZnO seed layer to lower the thermodynamic energy barrier for the initiation of the crystallization process since these seeds provide nucleation sites for the next reduction and growth process of 1D nanorods [20,29,30]. Therefore, before ZnO synthesis, a ZnO seed layer is formed on the surface simply by air oxidation of the zinc plates without using a detailed pre-coating step in this work. The melting point of zinc metal is ~420°C [28]. Thus, 300°C is chosen as a reasonable temperature for the thermal oxidation. Then, the substrates are annealed for two different durations (3 h and 6 h) to form a ZnO seed layer on the substrates.

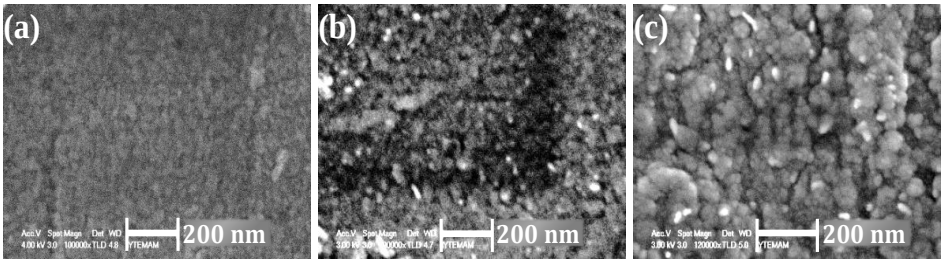

Fig. 2. SEM images of zinc substrate (a) after cleaning; and oxidized at 300°C in air for (b) 3 h and (c) 6 h

The surface morphology of zinc substrates before and after thermal oxidation is evaluated by SEM images, as given in Fig. 2. The surface of the zinc plate seems quite homogeneous (Fig. 2(a)) before annealing. After 3 h annealing, the tiny spherical ZnO seeds are covered over the surface, as shown in Fig. 2(b). The seeds have an average size of ~14±5 nm. When the duration is increased to 6 h, the seeds become readily apparent because of aggregation (Fig. 2(c)), and their sizes increase to ~21±9 nm. However, it seems that, nanorod growth is also initiated on these seeds at longer durations, as revealed from the existence of small thin rods (white shiny parts) observed in the SEM image of Fig. 2(c). The initiation of the scarcely distributed ZnO nanowires was also observed by Florica et al. [25] after thermal

treatment at 400°C for 12 h, and by Chuah and Hassan [31] at 500°C for 30 min. These types of structures will adversely affect the alignment of the nanorods in the growth stage. Furthermore, macro cracks are observed on the surface, and also the zinc plate is bent (no longer a flat surface) after 6 h. Therefore, annealing time is selected as 3 h for seeding the substrates before use.

3.3. Effect of Seed Layer Formation on ZnO Nanorod Growth

ZnO nanorods are grown on both seeded and non-seeded zinc surfaces to investigate the effect of the seed layer. The nanorods grown on seeded and non-seeded plates are shown in Fig. 3(a) and (b), respectively. When the seeded substrates are used, densely distributed and very short nanorods (Fig. 3(a)) are obtained with an average diameter and length of 51±12 nm and 112±17 nm, respectively. While the ZnO nanorods produced on the seeded surfaces grow perpendicular to the surface, randomly oriented rods are obtained on the non-seeded surfaces (Fig. 3(b)). Therefore, because of this inclined orientation, the number density of short rods in the absence of seeding (11.3×10^9 #/cm^2) is less than that of seeded ones (18.1×10^9 #/cm^2). Nevertheless, short rods with nearly similar sizes (D = 81±13 nm and L = 156±18 nm) are formed without seeding. On non-seeded surfaces, it seems that, the initial ZnO nuclei (seeds) are formed on the zinc plate more randomly at the beginning of the crystallization. Thereby, the aggregation of rods and also their misalignment evolves during the growth stage.

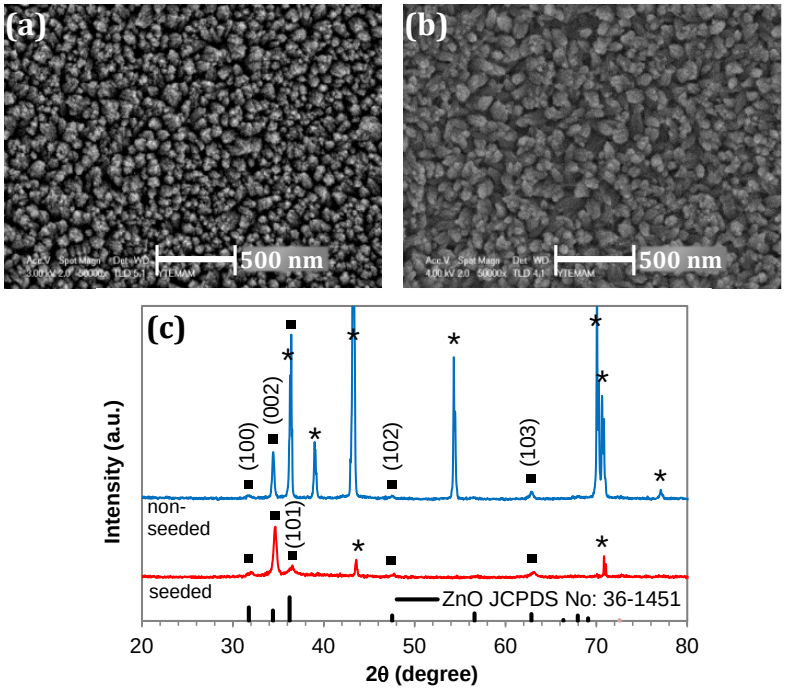

Fig. 3. SEM images of ZnO nanorods grown on (a) seeded and (b) non-seeded substrates; and (c) their corresponding XRD diffractograms ([Zn^{2+}] = 0.01 M, R = 10)

XRD analysis of the synthesized nanorods is given in Fig. 3(c) for both cases. Peaks of ZnO are shown by filled square (■). The diffraction peaks are well indexed with the diffraction pattern of ZnO standard with JCPDS card No: 36-1451, signifying that the synthesized ZnO rods are in hexagonal wurtzite structure [27]. The observed diffraction planes of ZnO for the samples are noted in Fig. 3(c). The peaks originated from the zinc substrate are denoted

by stars in the figure. No additional peaks are detected in the curves, showing the absence of impurities in the nanorods. The intensity of peaks coming from the zinc foil is high in non-seeded substrates, probably due to the misalignment of rods. Contrarily, the intensity of the (002) peak is higher than all other peaks for ZnO nanorods grown on seeded surfaces. This demonstrates the preferential growth of ZnO structures along the *c*-axis direction of the wurtzite unit cell (⟨0001⟩ basal plane of hexagonal rod) [11,28]. Thus, the intense (002) peak observed for seeded ones verifies the high degree of alignment of the resultant nanorods. The highest peak of short rods formed without seeding is in (101) direction, showing growth of both lateral and *c*-axis direction. Overall, it can be inferred that seeding of zinc substrates with a ZnO layer is a crucial preconditioning step to synthesize well-aligned ZnO nanorods.

3.4. Effect of [Zn^{2+}] in the Growth Solution

The changes in the morphology of the ZnO nanorods for different $Zn(NO_3)_2$ concentration are given in Fig. 4 at different magnifications. *R* is taken as constant at 10. With increasing Zn^{2+} concentration, the shape of the obtained structures changes from short and dense rods (0.01 M in Fig. 3(a)) to nanorods with tapering ends (Figs. 4(a-b)), and finally to nanorods having well-faceted hexagonal tops (0.15 M in Fig. 4(c)). Figs. 4(d-f) indicate that the rods are uniformly distributed all over the surface and the degree of verticality of the rods increases with Zn^{2+} concentration.

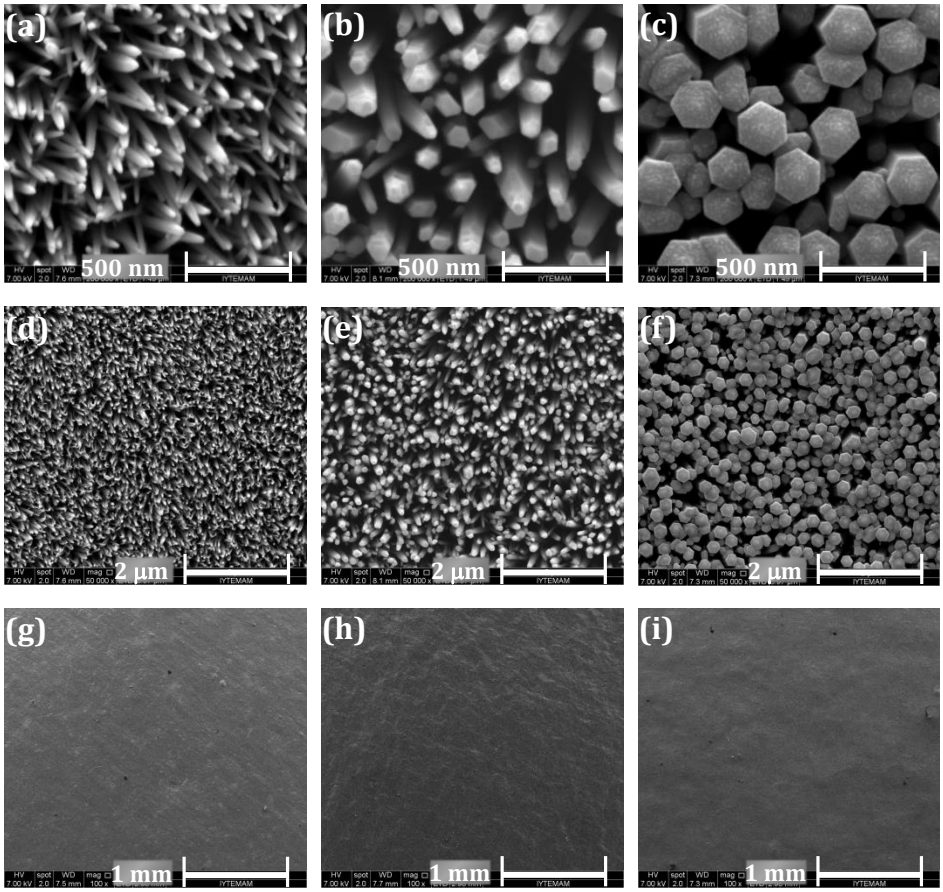

Fig. 4. SEM images of ZnO nanorods synthesized using [Zn^{2+}] of (a,d,g) 0.05 M, (b,e,h) 0.1 M and (c,f,i) 0.15 M, at different magnifications (R = 10)

The view of the coated substrates (~6 mm^2 surface area) in small magnifications is shown in Figs. 4(g-i). Figs. 4(g-i) reveal that nanorods are produced very homogeneously also in millimeter scale. There are no observable cracks or defects in that length scale.

The changes in the diameter, length, aspect ratio, and number density of nanorods are given in Table 2 for each concentration. The diameter of the nanorods increases from ~51 nm to ~257 nm with concentration, so their number density decreases from 18.1×10^9 #/cm^2 to 2.6×10^9 #/cm^2. The length so the aspect ratio of the rods rises up to [Zn^{2+}] = 0.1 M, at which highest values are attained. The maximum rod length of 5.52 μm and L/D ~ 51 is obtained. At [Zn^{2+}] = 0.15 M, the radial growth of rods (D = 257 nm, the biggest diameter in all concentration) and also clear hexagonal face formation at the top ends of the rods is more dominant. So, the growth in length direction is retarded at high Zn^{2+} concentrations.

Table 2. Morphology and dimensions of the ZnO nanorods obtained for different Zn^{2+} concentration at R = 10

	[Zn^{2+}] in the Growth Solution			
Nanorod property	0.01 M	0.05 M	0.10 M	0.15 M
Shape	Nanorods (short and dense)	Nanorods (tapering ends)	Nanorods (tapering ends)	Nanorods (hexagonal ends)
Orientation	Well-aligned	Well-aligned	Well-aligned	Well-aligned
Diameter, D (nm)	51±12	62±8	109±20	257±21
Length, L (μm)	0.11±0.02	1±0.11nm	5.52±0.21	4±0.61
Aspect ratio, L/D	2.2	16.1	50.5	15.6
Number density ($\times10^9$ #/cm^2)	18.1	13.3	6.1	2.6
D_c from XRD (nm)	21.7	38.6	59.0	36.5
FWHM of (002) peak (degree)	0.39	0.23	0.16	0.24

The crystal structures of the nanorods for different concentration of Zn^{2+} are examined using XRD analysis, given in Fig. 5. All peaks conform to the diffraction pattern of ZnO (JCPDS card no: 36-1451) and the synthesized nanorods have hexagonal wurtzite structure. The stars in the figure indicate the zinc coming from zinc foil. The (002) peak has the highest and the dominant intensity compared to other peaks, indicating that the dominant crystallographic growth direction of the nanorods is in the *c*-axis. Another peak at (101) direction is observed for the hexagonal rods formed in 0.15 M Zn^{2+} solution, showing the growth of rods both in lateral and perpendicular direction. The average crystallite sizes calculated using Eq. (1) and FWHM values measured from (002) peak are also noted in Table 2. An increase in D_c and a decrease in FWHM values signify that the crystallinity of ZnO nanorods increases up to 0.1 M and it decreases for 0.15 M along *c*-axis, probably due to the amount of imperfections in the crystal evolved with excess amount of Zn^{2+}. D_c (59 nm) and FWHM (0.16°) values for [Zn^{2+}] = 0.1 M agree well with the values obtained by Thein et al. (FWHM=0.125 and D_c=69.48 nm) for rod-shaped nanoparticles [32], and also by Karaduman Er (FWHM=0.251 and D_c=64.30 nm) for ZnO films [33].

The intensity of (002) diffraction plane (which represents the growth in *c*-axis) is displayed in Fig. 6 for different [Zn^{2+}]. The maximum intensity is detected at 0.1 M, thus verifying the SEM findings. (100), (101), (102) and (103) peaks of ZnO crystal are commonly used to exhibit the crystal growth directions other than the *c*-axis [24].

Therefore, the misalignment of nanorods is tried to be quantified by normalizing intensity of these peaks by the intensity of (002) peak [26], I/I(002).

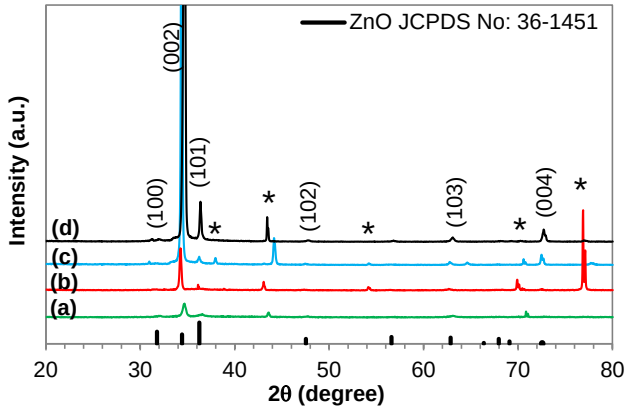

Fig. 5. XRD diffractograms of ZnO nanorods synthesized using [Zn^{2+}] of (a) 0.01 M, (b) 0.05 M, (c) 0.10 M, and (d) 0.15 M

The results are also shown in Fig. 6. The lowest normalized values (in other words, the highest alignment of rods) are observed at 0.1 M condition. This verifies the higher crystalline quality of rods and 1-dimensional growth of them compared to other concentrations. Therefore, 0.1 M is selected as the optimum zinc ion concentration. The cross-sectional view of the resultant nanorods at [Zn^{2+}] = 0.1 M and R = 10 is given in Fig. 7 to show their well-aligned structure.

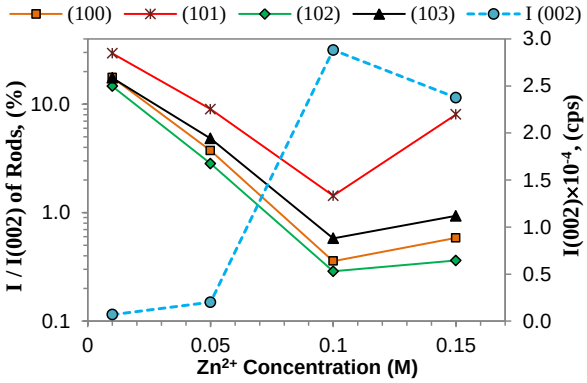

Fig. 6. Normalized XRD peaks of Fig. 5, by the intensity of (002) peak (I(002))

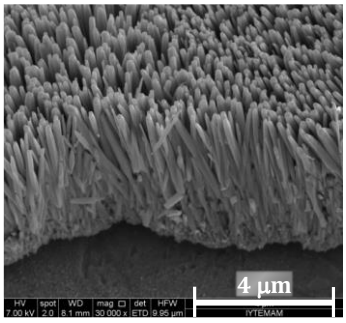

Fig. 7. Cross-sectional SEM view of ZnO nanorods

3.5. Effect of *R* Ratio in the Growth Solution

SEM images of nanorods synthesized at different R value ([Zn^{2+}] = 0.1 M) are given in Fig. 8 and their shape factors are summarized in Table 3. Well-aligned nanorods with tapering ends are obtained over the entire surface for R = 7 (Fig. 8(a)) and R = 10 (Fig. 4(b)). The rods having well-faceted and hexagonal symmetry are produced by further increasing R to 15 (Fig. 8(b)). Diameter of rods rises slightly from 71 nm (R = 7) to 121 nm (R = 15). However, a decrease in length of rods is detected after R > 10. When R = 20, the morphology of nanorods changes completely, and very dense and short rods stuck

together are observed (Fig. 8(c)). This is also observed by Yu et al. [17] for ZnO nanorods grown on ITO substrates, and they even cannot produce any particles on the ITO surface at high concentrations. This could be attributed to the excess amount of ammonia in the growth solution. Zn^{2+} forms stable complex by ammonia at high *R* ratios, which probably resulted in the quenching of nucleation and growth [18,20,21].

Table 3. Morphology and dimensions of the ZnO nanorods obtained for different *R* values at $[Zn^{2+}]$ = 0.10 M

	$R = n_{NH_3}/n_{Zn^{2+}}$			
Nanorod property	7	10	15	20
Shape	Nanorods (tapering ends)	Nanorods (tapering ends)	Nanorods (hexagonal ends)	Thin and very dense rods
Orientation	Well-aligned	Well-aligned	Well-aligned	Well-aligned
Diameter, D (nm)	71±16	109±20	121±18	25±3
Length, L (μm)	1.92±0.21	5.52±0.21	2.32±0.17	0.25±0.03
Aspect ratio, L/D	21.2	50.5	19.1	10.8
Number density ($\times 10^9$ #/cm^2)	9.7	6.1	5.7	56.7
D_c from XRD (nm)	40.4	59.0	37.7	23.2
FWHM of (002) peak (degree)	0.22	0.16	0.23	0.37

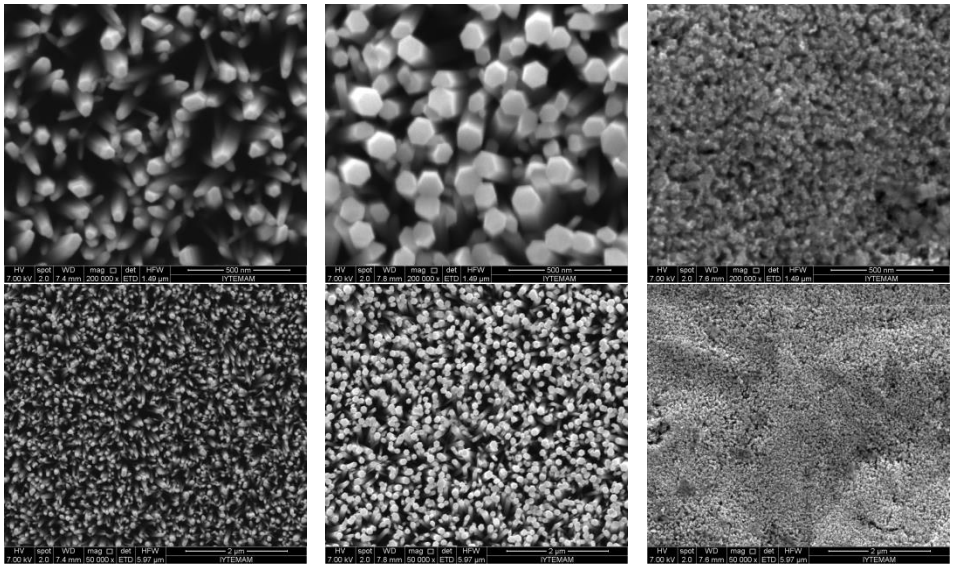

(a) (b) (c)

Fig. 8. SEM images of ZnO nanorods synthesized using $[Zn^{2+}]$ = 0.10 M, and (a) *R* = 7, (b) *R* = 15 and (c) *R* = 20 at different magnifications

XRD result (Fig. 9) revealed that the obtained coatings for all *R* values are ZnO with wurtzite crystal structures; and, the highest intensity peak belong to (002) plane except for *R* = 20. Also, no impurity in the samples is detected. The intensity of (002) peak and average size of crystallites decreases (FWHM value increases) from *R* = 10 to *R* = 20, denoting a decrease in the crystallinity of the rods. As the concentration of NH_3 is increased in the medium, the peak at (101) direction is started to evolve, showing growth of both lateral and perpendicular direction. (101) plane is the highest intensity peak at *R* = 20 and

the data confirms the SEM findings. Normalized peaks are also given in Fig. 10 to determine the degree of misalignment in the nanorods. The minimum I/I(002) values, that is the maximum verticality of rods, coincide at R = 7-10 range, which is compatible with the SEM results. The misalignment in rods increases abruptly for R > 15 and especially at R = 20, where the structure of rods are changed completely.

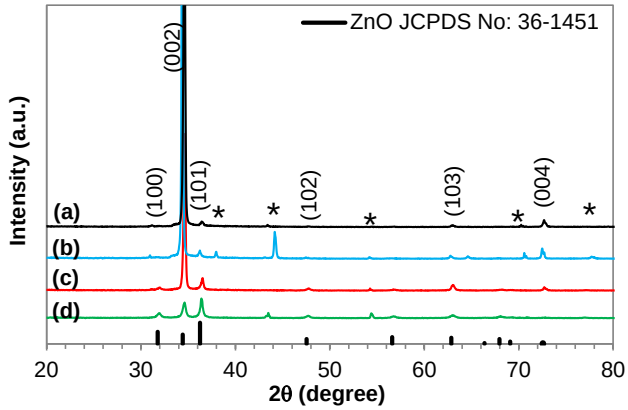

Fig. 9. XRD diffractograms of ZnO nanorods synthesized using [Zn^{2+}] = 0.10 M, and (a) R = 7, (b) R = 10, (c) R = 15, and (d) R = 20

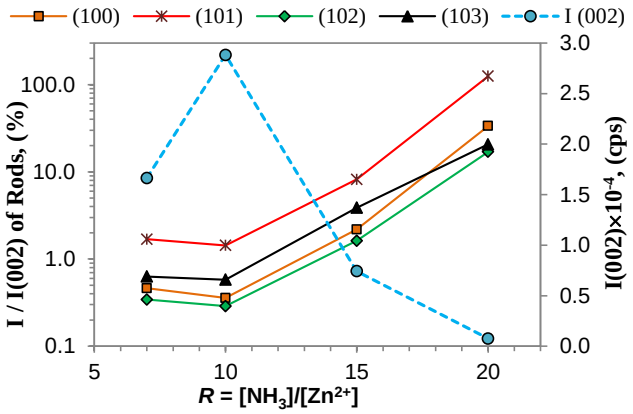

Fig. 10. Normalized XRD peaks of Fig. 8, by the intensity of (002) peak (I(002)) in the *c*-direction

4. Conclusions

In this study, 1D ZnO nanorod arrays were grown on zinc substrates by hydrothermal method in two steps. First, a ZnO seed layer was formed on zinc plates by thermal oxidation of the surfaces without deforming them. Then, ZnO nanorods were grown on these seeds within zinc–ammonia complex solution at a low temperature of 90°C and low durations (1.5 h). The listed parameters were investigated in detail to synthesize uniform and highly aligned ZnO nanorods: (i) the use of seeded and non-seeded substrates; (ii) concentration of $Zn(NO_3)_2$ in the bulk solution (0.01–0.15 M); and (iii) change of $NH_3/Zn(NO_3)_2$ mole ratio, R (7–20). As a conclusion,

- When seeded substrates were used in the reaction, the diameter of the nanorods obtained became smaller and orientation of the rods was more perpendicular to the

surface. Also, the number density of rods was higher because of compact configuration and verticality.

- Nanorods grown on non-seeded plates had random orientation, and they followed the counter of the surface. Therefore, seeding of the substrates is an important step to obtain highly aligned growth of 1D ZnO arrays.
- When $[Zn^{2+}]$ = 0.01 M in the reaction medium, short rods with high population density (18.1×10^9 #/cm^2) and low aspect ratios (~2) were formed all over the surfaces.
- With the increase in $[Zn^{2+}]$ from 0.01 M to 0.15 M, the diameter of the nanorods increased from 50 nm to 250 nm and length, from 110 nm to 5.5 μm. Nanorods with hexagonal structure and high verticality were achieved on seeded substrates and in $[Zn^{2+}]$ = 0.1 M growth solution.
- With the rise in R, misalignment of rods increased. Moreover, the use of excess amount of NH_3 (R = 20) caused the structure of the rods to change completely: from hexagonal ended long nanorods to short and thin rods stuck together.
- XRD analysis showed that all nanorods were ZnO with hexagonal wurtzite crystal structure. The highest intensity peak was detected at (002) direction, which is the 1D growth direction of rods.
- As a result of all parameter investigations, the optimum reaction medium was determined as $[Zn^{2+}]$ = 0.1 M and R = 10, at which the degree of misalignment of the nanorods was only approximately 0.5%.
- The results indicate that these simply grown nanorod arrays have a large potential to be used in photocatalytic and antibacterial applications due to their large exposed surface in polar (002)-direction, and also in electronic, solar cell and sensor applications because of their highly aligned 1D structure. In addition, this approach can be used in large-scale fabrication of nanostructured materials since it is a low temperature, simple technique and does not require a detailed pre-coating step for zinc substrates.

Acknowledgement

The authors acknowledge that this work was supported by the Scientific and Technological Research Council of Türkiye with the grant number of 110M403.

References

[1] Lee JH, Leu IC, Hon MH. Substrate effect on the growth of well-aligned ZnO nanorod arrays from aqueous solution. Journal of Crystal Growth, 2005; 275: e2069 - e2075. https://doi.org/10.1016/j.jcrysgro.2004.11.267

[2] Yu K, Jin Z, Liu X, Liu Z, Fu Y. Synthesis of size-tunable ZnO nanorod arrays from NH3.H2O/ZnNO3 solutions. Materials Letters, 2007; 61: 2775 - 2778. https://doi.org/10.1016/j.matlet.2006.10.029

[3] Le AT, Ahmadipour M, Pung S-Y. A review on ZnO-based piezoelectric nanogenerators: Synthesis, characterization techniques, performance enhancement and applications. Journal of Alloys and Compounds, 2020; 844: 156172. https://doi.org/10.1016/j.jallcom.2020.156172

[4] Chandana MR, Lavanya DR, Radha krushna BR, Daruka prasad B, Malleshappa J, Sharma SC, Joy FrD, Soundararajan P, Nagabhushana H. Effect of precursors on ZnO nanoparticles to enhance the level-III ridge details of LFPs and anti-counterfeiting applications. Materials Science in Semiconductor Processing, 2023; 167: 107749. https://doi.org/10.1016/j.mssp.2023.107749

[5] Yudasari N, Hardiansyah A, Herbani Y, Isnaeni, Suliyanti MM, Djuhana D. Single-step laser ablation synthesis of ZnO-Ag nanocomposites for broad-spectrum dye

photodegradation and bacterial photoinactivation. Journal of Photochemistry & Photobiology, A: Chemistry, 2023; 441: 114717. https://doi.org/10.1016/j.jphotochem.2023.114717
[6] Zhu D, Zheng Y, Xiong Y, Cui C, Ren F, Liu Y. In situ growth of S-doped ZnO thin film enabling dendrite-free zinc anode for high-performance aqueous zinc-ion batteries. Journal of Alloys and Compounds, 2022; 918: 165486. https://doi.org/10.1016/j.jallcom.2022.165486
[7] Sharma DK, Shukla S, Sharma KK, Kumar V. A review on ZnO: Fundamental properties and applications. Materials Today: Proceedings, 2022; 49(8): 3028-3035. https://doi.org/10.1016/j.matpr.2020.10.238
[8] Li Z, Huang X, Liu J, Li Y, Li G. Morphology control and transition of ZnO nanorod arrays by a simple hydrothermal method. Materials Letters, 2008; 62: 1503 - 1506. https://doi.org/10.1016/j.matlet.2007.09.011
[9] Hames Y, Alpaslan Z, Kösemen A, San SE, Yerli Y. Electrochemically grown ZnO nanorods for hybrid solar cell applications. Solar Energy, 2010; 84: 426 – 431. https://doi.org/10.1016/j.solener.2009.12.013
[10] Kakati N, Jee SH, Kim SH, Oh JY, Yoon YS. Thickness dependency of sol-gel derived ZnO thin films on gas sensing behaviors. Thin Solid Films, 2010; 519: 494 - 498. https://doi.org/10.1016/j.tsf.2010.08.005
[11] Torkamani R, Aslibeiki B. Bulk ZnO, nanoparticles, nanorods and thin film: A comparative study of structural, optical and photocatalytic properties. Journal of Crystal Growth, 2023; 618: 127317. https://doi.org/10.1016/j.jcrysgro.2023.127317
[12] Wang Z, Qian X, Yin J, Zhu Z. Large-scale fabrication of tower-like, flower-like, and tube-like ZnO arrays by a simple chemical solution route. Langmuir, 2004; 20: 3441 - 3448. https://doi.org/10.1021/la036098n
[13] Kaidashev EM, Lorenz M, von Wenckstern H, Rahm A, Semmelhack H-C, Han K-H, Benndorf G, Bundesmann C, Hochmuth H, Grundmann M. High electron mobility of epitaxial ZnO films on c-plane sapphire grown by multistep pulsed-laser deposition. Appl. Phys. Lett., 2003; 82: 3901 - 3903. https://doi.org/10.1063/1.1578694
[14] Ghosh R. Recent progress in piezotronic sensors based on one-dimensional zinc oxide nanostructures and its regularly ordered arrays: From design to application. Nano Energy, 2023; 113: 108606. https://doi.org/10.1016/j.nanoen.2023.108606
[15] Wei XH, Jie WJ, Huang W, Zhu J, Li YR. Effect of symmetry of substrate surfaces on the orientation and growth mode of ZnO films. Journal of Crystal Growth, 2009; 311: 2391 - 2396. https://doi.org/10.1016/j.jcrysgro.2009.02.021
[16] Yang Z, Luan C, Zhang W, Liu A, Tang S. Fabrication and optical properties of ZnO nanostructured thin films via mechanical oscillation and hydrothermal method. Thin Solid Films, 2008; 516: 5974 - 5980. https://doi.org/10.1016/j.tsf.2007.10.085
[17] Yu K, Jin Z, Liu X, Zhao J, Feng J. Shape alterations of ZnO nanocrystal arrays fabricated from NH3.H2O solutions. Applied Surface Science, 2007; 253: 4072 - 4078. https://doi.org/10.1016/j.apsusc.2006.09.001
[18] Yue S, Lu J, Zhang J. Controlled growth of well-aligned hierarchical ZnO arrays by a wet chemical method. Materials Letters, 2009; 63: 2149 - 2152. https://doi.org/10.1016/j.matlet.2009.06.055
[19] İkizler B. Preparation of single- and double-layer antireflective coatings by sol-gel method. Research on Engineering Structures and Materials, 2020; 6(1): 1-21.
[20] Baruah S, Dutta J. pH-dependent growth of zinc oxide nanorods. Journal of Crystal Growth, 2009; 311: 2549 - 2554. https://doi.org/10.1016/j.jcrysgro.2009.01.135
[21] Li Z, Huang X, Liu J, Li Y, Ji X, Li G. Growth and comparison of different morphologic ZnO nanorod arrays by a simple aqueous solution route. Materials Letters, 2007; 61: 4362 - 4365. https://doi.org/10.1016/j.matlet.2007.02.003
[22] Li C, Wang Y, Chen S, Zhang W, Wang Z, Hou Z. Enhanced photoelectrochemical performance based on conformal and uniform ZnO/ZnSe/CdSe heterostructures on Zn

foil substrate. International Journal of Hydrogen Energy, 2020; 45: 8257 - 8272. https://doi.org/10.1016/j.ijhydene.2020.01.069
[23] Yan C, Xue D. Solution growth of nano- to microscopic ZnO on Zn. Journal of Crystal Growth, 2008; 310: 1836 - 1840. https://doi.org/10.1016/j.jcrysgro.2007.10.060
[24] Torres FCG, López JLC, Rodríguez ASL, Gallardo PS, Morales ER, Hernández GP, Guillen JCD, Flores LLD. Sol-gel/hydrothermal synthesis of well-aligned ZnO nanorods. Boletín de la Sociedad Española de Cerámica y Vidrio. 2023; 62(4): 348-356. https://doi.org/10.1016/j.bsecv.2022.05.004
[25] Momeni M.M. One-step synthesis of ZnO nanowires on zinc foils and their photocatalytic properties. Indian Journal of Chemistry, 2016; 55A: 686 - 691.
[26] Florica C, Preda N, Costas A, Zgura I. Enculescu I. ZnO nanowires grown directly on zinc foils by thermal oxidation in air: Wetting and water adhesion properties. Materials Letters, 2016; 170: 156 - 159. https://doi.org/10.1016/j.matlet.2016.02.035
[27] İkizler B, Peker SM. Effect of the seed layer thickness on the stability of ZnO nanorod arrays. Thin Solid Films, 2014; 558: 149 - 159. https://doi.org/10.1016/j.tsf.2014.03.019
[28] Widyastuti E, Hsu JL, Lee YC. Insight on photocatalytic and photoinduced antimicrobial properties of ZnO thin films deposited by HiPIMS through thermal oxidation. Nanomaterials, 2022; 12: 463. https://doi.org/10.3390/nano12030463
[29] Vayssieres L, Keis K, Lindquist S-E, Hagfeldt A. Purpose-built anisotropic metal oxide material: 3D highly oriented microrod array of ZnO. Journal of Physical Chemistry B, 2001: 105: 3350 - 3352. https://doi.org/10.1021/jp010026s
[30] Greene LE, Law M, Tan DH, Montano M, Goldberger J, Somorjai G, Yang P. General route to vertical ZnO nanowire arrays using textured ZnO seeds. Nano Letters. 2005; 5(7): 1231-1236. https://doi.org/10.1021/nl050788p
[31] Chuah LS, Hassan Z. Thermal annealing effect on properties of Zn foils substrates. Materials Science Forum, 2015; 819: 215 - 219. https://doi.org/10.4028/www.scientific.net/MSF.819.215
[32] Thein MT, Chim JE, Pung S-Y, Pung Y-F. Highly UV light driven WOx@ZnO nanocomposites synthesized by liquid impregnation method. Journal of Industrial and Engineering Chemistry, 2017; 46: 119-129. https://doi.org/10.1016/j.jiec.2016.10.022
[33] Karaduman Er I. Development of ZnO sensors via succession ionic layer adsorption and reaction (SILAR) method for ppb level NO gas sensing. Research on Engineering Structures and Materials, 2021; 7(2): 259-272. https://doi.org/10.17515/resm2020.212ma0901